Cryst. Res. Technol. 52, No. 1, 1600223 (2017) / DOI 10.1002/crat.201600223

CRYSTAL Research & Technology

Original Paper

Identification of solid oxygen-containing Na-electrolytes: An assessment based on crystallographic and economic parameters

Falk Meutzner[1,*], *Wolfram Münchgesang*[1], *Tilmann Leisegang*[1,2], *Robert Schmid*[1], *Matthias Zschornak*[1], *Mateo Ureña de Vivanco*[1], *Alexander P. Shevchenko*[2], *Vladislav A. Blatov*[2], *and Dirk C. Meyer*[1]

Received 15 July 2016, revised 28 August 2016, accepted 31 August 2016
Published online 28 September 2016

We have scanned the inorganic crystal structure database using Voronoi-Dirichlet methodology for inorganic, crystalline, solid Na electrolytes and applied a total of nine different crystallographic and economic parameters in order to evaluate the potential of each material. Especially for stationary electrochemical energy storage — used to counteract the capricious nature of renewable energy sources and momentary variations of energy consumption — Na-based chemistries have a considerable market share. They rely on solid Na electrolytes separating the Na and S electrode compartments. We used data generated from the currently widest-spread Na electrolytes to lay a foundation for the crystallographic data mining and Voronoi-Dirichlet partitioning of the database. The structural data is the basis for the calculation of the above-mentioned parameters. We introduced an evaluation and scoring scheme to systematise the results and — depending on the weighting scheme — point towards the most promising materials. Aluminosilicates and transition metal oxides seem especially interesting but, depending on the weighting, any of the more than 400 candidates could be the next-generation solid Na electrolyte.

1 Introduction

1.1 Energy and economy

Electrical energy has become one of the most versatilely applicable forms of energy since the 19th century. In 2015, about 24 PWh of electrical energy were produced worldwide, numbers on the rise [1]. Besides the increasing demand of energy supply in portable devices and for electromobility, the growing share of renewable or alternative energy on the total energy generation drives the need for efficient stationary energy storages. Furthermore, these systems can also be used to buffer momentary variations of electricity in order to ensure the malfunction-free supply of electrical energy. Due to failure of high-tech industrial equipment, costs of about 188 billion dollars per year were estimated for the US business [2].

Numerous technologies for electrical energy storage are employed today [3] and about 12 GWh are stored electrochemically. In total, more than 100 different electrochemical technologies are known. The Pb-acid, Li-ion, Ni-metal-hydride, NiCd and other technologies, such as redox-flow and sodium-sulphur (Na-S) have the highest impact. This is also due to their low criticality in terms of their availability as raw materials [4]. Up to now, considerable progress has been made in electrochemical energy storage technology, both through continued improvement of specific electrochemical systems and the development and introduction of new chemistries. Nevertheless, there is no one 'ideal' battery regarding cost per kWh, environmental sustainability, toxicity, recyclability, and safety that gives optimum performance under all operating conditions [5].

For long-term, large-scale energy storage applications in the 100 MW range there are several promising technologies on a commercial scale [3]. Besides the pumped hydroelectric energy storage (PHES), the Na-S battery technology accounts for the largest market share

* Corresponding author: e-mail falk.meutzner@physik.tu-freiberg.de, Phone: +49 3731 419 6168, Fax: +49 3731 419 6167
[1] TU Bergakademie Freiberg, Institut für Experimentelle Physik, Leipziger Straße 23, 09596 Freiberg, Germany
[2] Samara National Research University named after academician S.P. Korolyev, Moskovskoye Shosse 34, 443086 Samara, Russia

and is therefore of global interest [6]. Accordingly, up to now, more than 155 systems comprising a total power of ca. 340 MW are installed worldwide.

Ford Motor Company first developed the Na-S battery in the 1960s [7]. This was possible due to the discovery of β-alumina, which shows a high conductivity for Na ions at the operating temperature of 300 °C [8]. It was used by Ford for electric vehicles in the 1990s. NGK Insulators Ltd. from Japan developed β-alumina-based ceramic electrolytes and further improved the concept for commercialisation as an advanced energy-storage technology in cooperation with Tokyo Electric Power Company (TEPCO) [2, 9]. In April 2003, NGK launched production on a commercial scale [10]. Today, Japan, with more than 140 systems installed, is the market leader [6].

In the Na-S technology, the separator has to work as a solid electrolyte in order to prevent direct electron transfer between Na and S on the one hand and to allow ion flow as the basis for energy delivery on the other hand. Temperatures of around 300 °C are necessary for normal operation of high-temperature Na-S batteries so that high thermal stability is required for the separator [11]. Further favourable properties of ceramic separators/solid electrolytes can be found elsewhere [12]. With regard to reported accidents and the expected strong growth of the separator and solid electrolyte market [13], such materials are of great importance, in particular to ensure safe battery systems. Separators/solid electrolytes should thus be designed such that they are not the rate-limiting component in an electrochemical cell by hindering ion flow which influences the charge/discharge rate, cell temperature, obtainable power, and cycle life of the whole electrochemical cell. For high-temperature Na-S batteries, only inorganic ceramic, glass-ceramic (e.g. Na_3PS_4) or glass electrolytes can be used due to the high operation temperatures and the intense reaction between Na and S at these temperatures [11, 14, 15].

1.2 Crystallography

As taken from Ref. [16], the best-conducting crystalline solid Na-ion electrolytes known so far can be categorised into three different main groups (β-alumina, NaSICon and Na rare-earth silicates) showing very similar, comparably high conductivities for Na^+ (approx. 10^{-3} S/cm at room temperature, around (10^{-2}–10^{0}) S/cm at 300 °C).

The β- and β''-alumina structures comprise alternating, closely packed Al-O spinel type blocks bonded to each other via a loosely packed Na-containing conduction layer. β- and β''-alumina compounds differ in stoichiometry and stacking sequence of oxygen ions across the conduction layer. In these layers, the intercalated Na^+ ions can migrate in two dimensions along the paths of the hexagonal lattice via existing vacancies generated by the non-stoichiometry of the overall compound [17, 18]. Both structure types are well-conducting but in the major part of literature, Na β''-alumina is reported best. The conduction network is based on a system of sites labelled Beevers-Ross (BR: 2/3, 1/3, 1/4), anti-Beevers-Ross (aBR: e.g. 0.1117, 0.2234, 1/4) and mid-Oxygen position (mO: 0.3333, 0.1667, 1/4). The latter is an important site during the conduction process and is not occupied in equilibrium. In the case of Na β''-alumina, BR and aBR are merged into one symmetrically equivalent site and the space group changes from $P6_3/mmc$ (β-alumina) to $R\bar{3}m$ (β''-alumina). The non-stoichiometry of the compound and thus the crystal structure are decisive for ion transport. In literature, a maximum conductivity of $3.6 \cdot 10^{-1}$ S/cm for polycrystalline and 1 S/cm for single crystalline materials at 300 °C is reported [19, 20]. At ambient conditions, single crystals still exhibit an ion conductivity of $(1.4–4.0) \cdot 10^{-2}$ S/cm, while the commercially available polycrystalline β''-alumina manufactured by Ionotec is characterised by $1.7 \cdot 10^{-3}$ S/cm [21, 22].

'NaSICon' (Na Super Ionic CONductor), discovered by Hong and Goodenough et al. [23], exhibits a structure composed of silicate/phosphate tetrahedra linked by metal ions, Zr^{4+} in this case, preferring octahedral coordination. The generalised formula is $Na_{1+x}Zr_2Si_xP_{3-x}O_{12}$ ($0 \leq x \leq 3$). The NaSICon structure is rhombohedral but shows an orthorhombic distortion for $1.8 < x < 2.2$, where conductivity excels. Built up by a 3D 'skeleton-like' structure, Na occupies 3D-connected interstitial positions in the 3D framework. The conduction path is described to proceed between two Na positions via an intermediate site called 'mid-Na'. This position is not occupied in an as-produced sample at equilibrium but was found to be important for the actual conduction process similar to the above-mentioned mO site [24].

The Na rare-earth silicate group (NaRES) is another slightly less-known superionic conductor built from a complex 3D matrix of silicate tetrahedra and rare-earth-oxygen octahedra sharing corners. They build up hexagonal, ring-like structures that are stacked upon each other, incorporating structurally bound NaO_6 octahedra. For the best conducting phase of this group, $Na_5RESi_4O_{12}$, the actual conduction path is still under discussion. The most prominent mechanism is described by a 1D path of two inequivalent Na sites showing no bottle-neck between them [25]. Another distinct Na position may be a possible link between those 1D

CRYSTAL Research & Technology

channels resulting in a 3D conduction that is anticipated to be suppressed.

The disadvantage of these materials is the comparably high technological complexity and thus manufacturing costs. Further problems comprise their brittleness, complexity of thin film production, energy density optimisation, and poor stability. New materials can have a high potential in lowering costs and technological complexity, increasing low temperature performance and chemical stability. A first assessment was made [26] only addressing ternary compounds with Na and O. In this study, the assessment is extended so that now all compounds — comprising at least Na and O — are taken into account. Crystallographic and economic parameters have been evaluated and are discussed in the course of the work.

2 Methodology

2.1 Voronoi-Dirichlet partitioning

Voronoi-Dirichlet partitioning geometrically subdivides a space filled with points. Each point is assigned a polyhedron that describes the space closer to this point than to any other point. Voronoi-Dirichlet polyhedra (VDP) can partition and describe crystal structures into atomic domains. Each VDP is characterised by its volume, faces, vertices, and edges, which can be chemically interpreted as atomic sizes, bond strengths, structure-immanent voids, and connections between these voids, respectively [27].

The programme package 'ToposPro' is a multifunctional tool for crystallographic analysis which enables the application of Voronoi-Dirichlet partitioning for crystallographic compounds and whole crystallographic databases through built-in database-handling routines [28]. ToposPro introduces a set of geometric parameters for the numerical evaluation of VDP.

For the analysis of ion conductivity in this study, the most important values are the radius of the spherical domain r_{SD} — the radius of a virtual sphere with the volume of the VDP — and the solid angle Ω — the percentage of a VDP face projected on a unit sphere. It is used as a measure for bond strength. The larger this value, the closer the two atoms connected by this face, the more they interact with each other. In this context, it separates strong from weak bonds: Ω_{min} is defined as the smallest solid angle that still characterises a strong bond.

Another important VDP property is that its vertices and edges represent the sets of points most distant from the framework atoms. This means that they can be assigned to centres of voids and channel lines, respectively. Determining VDPs for void centres one can discard too small voids for being unavailable for mobile cations and, finally, construct the migration map. For this work, we chose to neglect channel radii as discussed in Ref. [29] since we intend to avoid mixing the idea of soft spheres — applied to the whole coordination sphere of an atom (r_{SD}) — and a hard sphere consideration — for those atoms directly constituting the channel (R_{chan}). Furthermore, the larger the r_{SD} values for the channel-connected voids, the larger the channel radii [26].

In order to analyse a crystal structure for a possible ion conduction with VDP, the compound needs to comprise the to-be-conducted cation — Na^+ — and an arrangement of anions — here O^{2-} — as well as additional metal ions M^{m+}. In such a material, $Na_xM_yO_z$, the vertices of the VDP around each M and O atom propose all structure-immanent voids of the M_yO_z framework. As the structure should be analysed for all sites that could host Na ions, structure-immanent Na ions need to be ignored and all remaining sites have to be calculated. Two conditions must be fulfilled for a compound to show ion conductivity referring to the Voronoi-Dirichlet partitioning:

1. 'Determination': Both voids and channels need to be determined by anions only. If one of the void-constituting atoms is a cation, Coulomb repulsion could give an energy barrier too large for another cation to enter this site or channel. For this purpose, all voids showing void-cation solid angles larger than Ω_{min} need to be neglected.
2. 'Comparison': The geometrical data of the voids is compared to expected values: r_{SD} needs to be at least as large as the data-mined value for Na in an O environment.

The determined void-channel system is only consistent with the VDP approach if both conditions are fulfilled [30]. For a more detailed description of the method and nomenclature, see Ref. [26]. A graphical representation the methodology is depicted in figure 1.

Voronoi-Dirichlet partitioning works most reliably for structures of higher symmetry and only if all respective neighbours are of the same chemical element. The second condition is satisfied, since determination needs to be considered for every void, anyway: there shall be only O next neighbours to a void. In low-symmetry structures, VDP could create highly complex void patterns and void clusters that are very difficult to interpret. We developed a new void-handling algorithm and implemented it in ToposPro. It merges all voids connected by VDP edges smaller than a specified value, here 1 Å, into their geometric centre. This simplification helps interpreting the

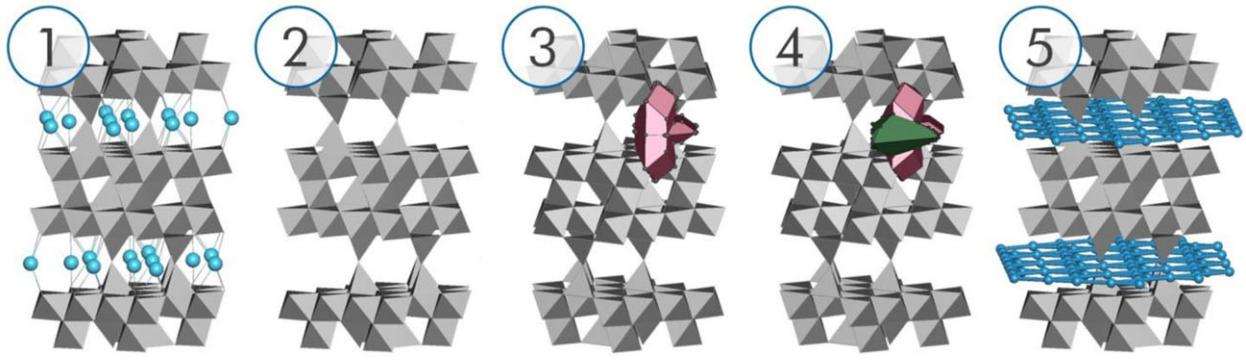

Fig. 1 Graphical demonstration of the VDP approach for Na β-alumina (ICSD-# 9144). From the structure (1) all Na ions (light blue) are ignored (2) and the VDP of all remaining atomic sites (selection in red) are calculated (3). For each of these VDP's vertices, a further VDP (green) is constructed (4) and compared to data-mined values in order to generate the conduction path (blue) (5).

results and accelerates the analysis done after the actual Voronoi-Dirichlet partitioning greatly.

2.2 Crystallographic and economic parameters

For our study, three main aspects were considered: Crystallography, electrochemistry, and economy. The crystallography of the (crystalline) material determines the energetic landscape of the ion that migrates through the compound. The coordination chemistry of each point within the conduction network needs to match energetically and the framework should be stable enough to allow for migration without collapsing.

The energetics of the material are also translated into its electrochemistry — the conductivity for ions and electrons as well as possible intercalation or decomposition potentials. Basically, all identified materials could also serve as intercalation electrodes for either the positive or negative side. The main differences between ion conductors and electrodes are, firstly, electronic conduction — electrodes need to be electronically conducting; solid electrolytes are insulator — and secondly, readily available oxidisable/reducible ions in the structure — none for electrolytes, at least one for electrodes. The latter can be determined by scanning the structure for ions showing multiple oxidation states. The former is difficult to obtain from crystallographic databases and should be either tested or calculated (e.g. by density functional theory (DFT)). Electronic conduction is the basic requirement for electrodes, since an insulator with multivalent ions cannot act as an electrode.

In our study, economy describes the availability, abundance, and price of the material for a subsequent industrial utilisation.

For the assessment, we collected a variety of parameters that were classified into crystallographic and economic factors. We assigned a score for each number in order to rate the material. By summing up all the points we found the most promising materials as those with most points. The parameters, their evaluation, and meaning are as follows:

2.2.1 Crystallographic parameters

sr: The standard deviation of the mean value of r_{SD} of all the voids constituting the proposed conduction network: this value is used as a first measure of the smoothness of the energetic landscape and thus the conductivity — the smaller the differences of the sizes of the conduction network sites, the smaller the expected differences in their energy.

ma: Dimensionality of the matrix: the matrix is defined as all the non-Na atoms in the structure as well as all those Na ions that are further than 1 Å from a void constituting the conduction network. The matrix builds up the framework for the supposed ion conduction (see figure 2). The higher the dimensionality of the matrix, the better. Abstractly speaking, VDP consider a system where the conducting ions could be described as a liquid inside of a framework. If the structural motifs of the matrix are not connected to each other, the conduction system instead would hold the system together. Hence, stability is questionable, since the cohesion of this phase is not assured if the conduction system is 'liquid-like'. For these cases, stability needs to be addressed for example with DFT.

dm: Dimensionality of the conduction network: the higher the dimensionality, the better. Crystallographically speaking, this increases the possible conduction paths and makes blocked tunnels less problematic. Higher-dimensional conduction network compounds

CRYSTAL Research & Technology

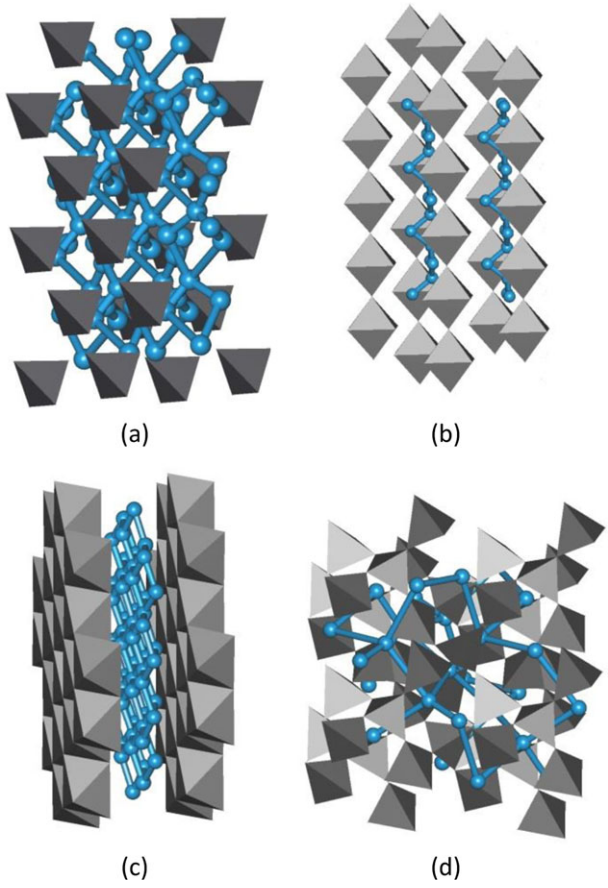

Fig. 2 Possible matrix dimensionalities (grey polyhedra: matrix; blue network: conduction network): (a) 0D (with 3D conduction network), (b) 1D (with 1D conduction network), (c) 2D (with 2D conduction network), and (d) 3D (with 3D conduction network).

have the advantage of enabling the deployment of polycrystalline materials (see figure 2).

sy: Crystal class: the higher the symmetry of the crystal class, the better. Here, the cubic class and those closest to it should be best-suited because their high intrinsic symmetry allows for multitudes of energetically equal positions (per Wyckoff sites), which is not expected (albeit not impossible) for triclinic and monoclinic candidates.

ms: Division of the sum of the multiplicities m of all void sites i (m_i) constituting the identified conduction network and the squared amount i^2 of these sites according to: $ms = \frac{\sum_i m_i}{i^2}$: every Wyckoff site with the same coordinate triplet (crystallographic orbit) has the same energy. Therefore, in order to create a uniform energy profile, few Wyckoff sites of high multiplicities are best-suited. In order to pronounce that few sites with high multiplicities are better than a multitude of low/high-multiplicity sites, the amount of voids is accentuated by squaring it. This value should be as high as possible.

oc: Mean occupancy of all Na sites in the identified conduction network: for this rating parameter, the mean occupancy of all Na sites j that are closer than 1 Å to a void constituting the conduction network is determined as $oc = \frac{\sum_j p_j \cdot m_j}{\sum_j m_j}$, where p denotes the site occupancy. The hopping of ions between sites is best achieved if there is a vacant site to hop onto [31]. For this study we presume that for ion conduction, the lower the occupancy of ions inside of the conduction channel, the better. Coordinative movement, which can also happen with fully occupied sites ($oc = 1$) while travelling through the bulk, may also be possible but is usually energetically less favourable.

2.2.2 Economic parameters

cr: Highest criticality of a constituent (chemical element) of the compound in question: the rating is based on the data of the 'Critical Raw Materials Group' of the European Union [4]. Criticality summarises and tries to quantify different sub-items of supply risk and technological/economic importance into one number. There are different systems and point of views — criticality is different for every region it is formulated for. We read out the numerical values for 'supply risk' and 'consequences of supply disruptions' for the European Union from figure 9b in Ref. [4], multiplied and square rooted them. We recorded the maximum criticality of all elements in every compound. If an element is not included in the reference, we estimated its values. There should be as few critical elements in the compound as possible.

pr: virtual price of the compound: we calculated it as $pr = \frac{u \cdot \sum_n M_n \cdot p_n \cdot m_n \cdot C_n}{V_{UC}}$, where u is the unified atomic mass unit, M_n and C_n are the molar mass and the price per gram of every site n in the structure, respectively, V_{UC} is the volume of the unit cell of the corresponding structure. For this study, we gathered the prices of the elements from different sources (see supplementary material). It is a crude approximation but will show trends. The more expensive the elements constituting a material, the more expensive it will become. The actual price could be higher or lower depending on the amount of energy needed for the synthesis and if materials for the synthesis are readily available. This value should be as low as possible.

de: The X-ray density of the compound: it is calculated as $\rho = \frac{u \cdot \sum_n M_n \cdot p_n \cdot m_n}{V_{UC}}$. In most cases, a low density is favourable for electrochemical applications since it lowers the general weight and thus increases the specific

energy of the system. There are cases, where high densities are no disadvantage — especially where volume is more important than weight — but for this study, we deemed lower densities more important.

For more details on element data and the full data set of all compounds, see the supplementary material.

3 Procedure

3.1 Data mining

First, all compounds comprising at least Na and O were filtered from the ICSD 16/1 [32]: 11,004 out of 183,804 entries. After all duplicates were deleted (9,152 remaining), all compounds whose chemical formula did not match the composition of the atomic positions were deleted as well, resulting in 5,541 compounds. In figure 3 the general handling and processing of the data up to the results is visualised.

In order to data mine only from well-defined standards, compounds showing no substitutional disorder on any crystallographic site were chosen (2,041 compounds). During the data mining, some compounds were omitted due to non-standard acquisition temperature/pressure or inconsistencies with the bulk of the data (8 compounds).

The most important data-mined value is the r_{SD} of Na in a pure oxygen coordination which amounts to $r_{SD} = (1.523 \pm 0.040)$ Å. This is slightly lower than previously determined [26] — probably through the usage of only non-disordered compounds. The difference to single coordination numbers is only small (CN6: (1.518 ± 0.046) Å, CN8: (1.523 ± 0.038) Å and within standard deviation.

In order to distinguish strong from weak bonds, the solid-angle threshold Ω_{min} was revisited. The solid angles of all common VDP faces between Na and any metal atom (non-chalcogen, non-halogen atoms) exhibit a distinct border between direct and indirect contacts. This yields a $\Omega_{min} = 5\%$ which is higher than previously determined [26] because only non-disordered structures were filtered in this study. For Na-cation faces with a higher Ω, a strong bond can be assumed. Due to Coulomb repulsion these sites should be avoided.

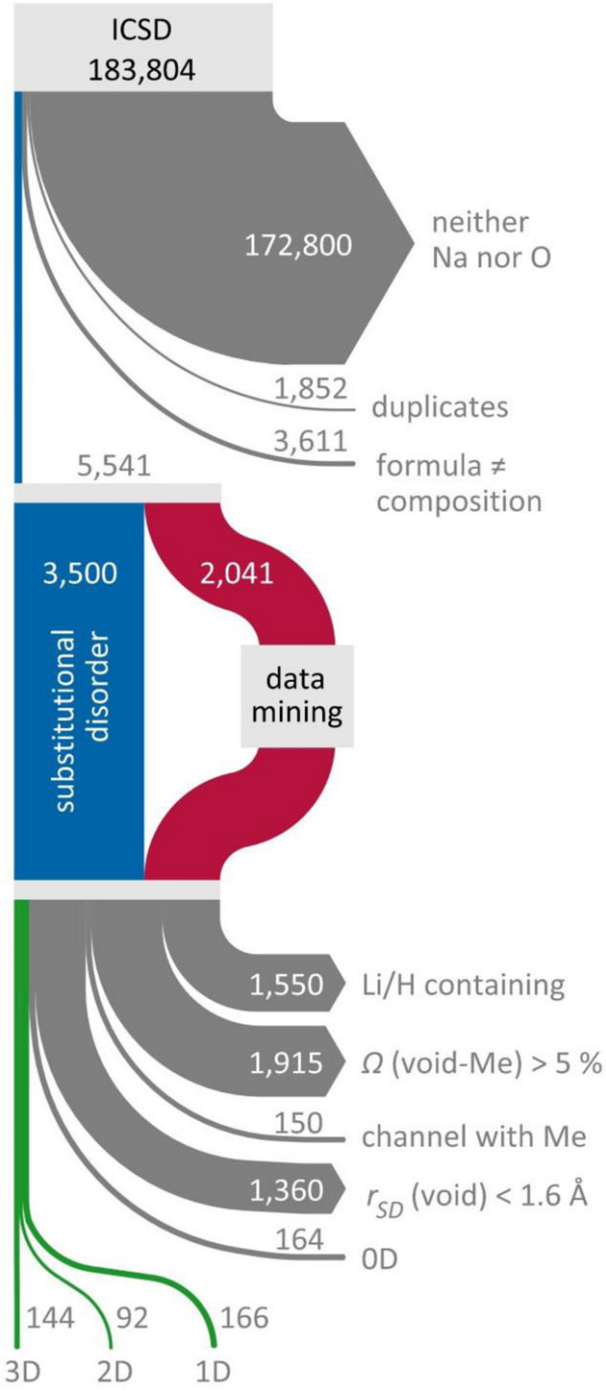

Fig. 3 Graphical representation of the data handling and processing as well as obtained most promising candidates for solid electrolytes.

3.2 Constraints — well-known solid Na-ion electrolytes

We applied these new values to the three best-known solid Na electrolytes already mentioned in the introduction:

1. In the ß''-alumina structure (based on ICSD-# 201178) all voids important for the conduction process are identified by VDP. In fact, the significance check alone (remove all voids with void-metal solid angles larger than 5%) already yields the full

CRYSTAL Research & Technology

migration path described by two voids corresponding to the BR/aBR site and the mO site in-between. The corresponding r_{SD} values are comparably high with values of 1.768 Å and 1.744 Å, respectively. The good conduction behaviour could be credited to the low deviation of site sizes.

2. The NaSICon structure has already been analysed with VDP [30]. The system of three obtained voids is in full agreement with the literature description encompassing two inequivalent Na sites and a mid-Na site. The r_{SD} values (based on ICSD-# 62383) are again rather large but smaller than for ß''-alumina: 1.711 Å, 1.603 Å, and 1.675 Å, respectively. One Na position is quite different in size in comparison to the other positions. This may translate into an energetically less smooth surface for the conduction path. This hop may represent the conductivity-limiting step. NaSICon is comparable in conduction and activation barriers to ß''-alumina.
3. The VDP analysis of the NaRES structure (based on ICSD-# 20271) is not as unambiguous as for the above-described compounds. The solid angle principle extracts thirteen voids. Especially those concentrated in the area inside of the silicate rings show lower r_{SD} values than the rest, i.e. smaller than 1.6 Å. By excluding all voids smaller than 1.605 Å, the 1D channel reported in literature is formed. The resulting voids range from 1.633 Å to 1.708 Å which is very similar to NaSICon. A 3D network would be enabled by allowing voids smaller than 1.605 Å.

The biggest problem of this collection is a difficult and missing assignment of structure and conductivity data since most of the information collected electrochemically has not been thoroughly associated to crystallographically analysed compounds and vice versa. The compounds discussed for each group have been chosen arbitrarily, albeit in the most careful fashion. Especially NaSICon shows a large variety of stoichiometries which is why a compound in the 'high-conductivity' range was chosen.

For the majority of the materials mentioned in Ref. [16] no crystallographic data was collected. Especially for the materials systematised under the 'Brucite-like' structures, conductivity data is presented without structural information. For this reason, we used the structural data of $Na_{0.68}Ni_{0.34}Ti_{0.66}O_2$ from Ref. [33] and modified it according to Ref. [34] to model the structure that is incompletely described in the former. The new data does not completely match the calculated value for the density — no site description is given in Ref. [33]. We could not identify a conduction path by Voronoi-Dirichlet partitioning. The site occupied by Na seems fairly small compared to both the data-mined value and the values found in the aforementioned examples. Either the diffusion mechanism in this system is different to the mechanism of the other three materials and not describable with VDP or the structure solution is inaccurate. Due to the lack of matching data sets for crystallographic and electrochemical analysis, a further examination of these compounds is not possible at this point.

To summarise, by first sorting out all voids with solid angles larger than 5% to non-oxygen-atoms; second, all channels with non-oxygen constituting atoms; and third all voids of $r_{SD} < 1.6$ Å, those voids remaining are similar to the conduction system sites of superionic Na conductors. If they percolate, as is the case for the three examples, the structure should exhibit good Na^+ conductivity according to Voronoi-Dirichlet partitioning.

4 Results

4.1 Voronoi-Dirichlet partitioning

From the aforementioned database of 5,541 compounds (including again compounds with disorder on crystallographic sites; figure 3), we omitted all those entries containing hydrogen (4,231 left) and lithium (3,991 left). Due to their chemical similarity and smaller radius, we expect a more preferable diffusion for those elements over Na.

By filtering all voids according to the determination and comparison principles (see last paragraph Sec. 3.2), a subset of voids is yielded for each compound. Non-connected or only singly-connected voids are deleted. Sites mainly occupied by Na are treated as 'full' Na sites by ToposPro, which is why we deleted all voids closer than 1 Å to a substitutionally disordered site. If there are non-Na ions in the conduction network, transport may either get blocked or at least slowed down as in the mixed-alkali effect [35, 36].

Afterwards, a dimensionality determination of the void system into tunnels (1D), planes (2D) and networks (3D) is carried out using ToposPro, resulting in the numbers presented in Table 1. We ignored all compounds with only non-percolating circles (0D dimensionality).

All 402 candidates with a 1D–3D void-network dimensionality satisfy the conditions described in Sec. 3.2. From a VDP point of view, all these materials are potential Na super ion conductors. In order to find the most promising candidates, we decreased this number by first omitting all entries containing either Be, Tc or elements of $Z > 84$ (radioactive elements are technologically and environmentally difficult to handle; 23 items). We

Table 1 Summary of all compounds with infinitely connected voids as determined by Voronoi-Dirichlet partitioning.

$N_{elements}$	1D	2D	3D	Sum
2	0	0	1	1
3	34	27	33	94
4	87	42	72	201
5	26	22	32	80
6	17	1	4	22
7+	2	0	2	4
sum	166	92	144	402

Table 2 Thresholds for the given score points in this work. If the condition in the field is fulfilled the amount of score points is credited to the compound (see Sec. 2.2 for further explanation). hex.: hexagonal; trig.: trigonal; tetra.: tetragonal; ortho.: orthorhombic; mono.: monoclinic; tricl.: triclinic).

score	5	4	3	2	1	0
sr (Å)	<0.01	<0.02	<0.03	<0.05	<0.075	>0.075
ma	3D		2D		1D	(0D)
dm	3D		2D		1D	0D
sy	cubic	hex./ trig.	tetra.	ortho.	mono.	tricl.
ms	>6	>4	>3	>2	>0.8	<0.8
oc	<0.3	<0.6	<0.8	<1	1	0
cr	<2.5	<4	<5	<6	<7	>7
pr (€/cm³)	<10	<50	<100	<500	<1,000	>1,000
de (g/cm³)	<1.7	<2.5	<3.2	<4	<5.5	>5.5

neglected the binary compound as it is a high-pressure material. Furthermore, to avoid any mixed-alkali effect, we left out all compounds containing any alkali-element other than Na as well (15).

From an energetic point of view, a flat energy landscape for the Na ions moving through the void system translates into low barriers. Too large voids are unlikely to conduct well. Presumably, the Na ion's charge would not be equilibrated for all spatial directions, increasing the energy of the ion. Therefore, all compounds with a mean r_{SD} larger than 2 Å (inner surface) and standard deviations larger than 0.1 Å (smooth energy landscape) are omitted (70 candidates).

In some cases there are Na sites further than 1 Å away from a void. We assume that these Na ions will not migrate. All compounds comprising only this kind of Na sites were taken out. A compound where Na needs to be inserted is not necessarily stable because of added charge (33 candidates). Similarly, if the matrix has a dimensionality of 0, stability is questionable (23 items).

We decided not to exclude compounds bearing multivalent ions as possible electrode candidates from the list since electronic conduction has to be elucidated first. Nevertheless, we included information on whether a multivalent ion is present in the structure in the list (supplementary material).

All parameters described in Sec. 2.2 were calculated for each structure. Each criterion was credited with a maximum of five points (see Tables 2 and 3). By summing these, a maximum of 45 points can be achieved for one compound. We chose the thresholds for this evaluation in a way to split the data into equal shares. The highest amount of points reached for the selected candidates is 34, the lowest 9.

When the algorithm is applied to all 402 compounds, many β- and β''-aluminas, NaSICons and NaRES structures are revealed. The algorithm deems these materials — with highly symmetric structures; consisting mainly of Al, Si, and P — to be good ion conductors. A total of 30 β- and β''-alumina-like structures, 19 NaSICons (with phosphate, silicate, and molybdate groups), and 8 NaRES-like structures were identified. As these structures are already well-known for their conduction performance, they are not explicitly recorded here. Interestingly, every compound with the space group $P6_3/mmc$ is a β-, every $R\bar{3}m$ a β''-alumina and every $R\bar{3}c$ a NaSICon or NaRES structure. Not all candidates identified in our previous work [26] were detected again with the new approach. For this work, the threshold values for r_{SD} have been significantly increased to represent values for already well-known conductors which is why a large number of the formerly identified materials do not show up.

Among the highest-scoring materials (27 with 34–27 score points) there are 16 aluminosilicates (8 (tri)nephelines, 6 natrolites, 1 sodalite, 1 cristobalite) that are very similar to each other and in general represent a very large group within the results. These materials show 'skeleton-like' structures and are described as zeolites and 'metal-organic-framework-like' compounds. Hence, it is not surprising — Al and Si are very abundant, technologically well-established, and light — that these materials have high scores. Only one phase with a measured Na-ion conductivity besides the well-known

Table 3 Selection of the best-rated materials showing the score — ranging from 0 to 5 (see Table 2) — for each single category as well as the sum of all categories. For an explanation of the categories see Sec. 2.2. The dimensionality of the matrix is 3D (corresponding to 5 points) for each compound and therefore left out. For the exact data and values, please refer to the supplementary material. Compounds very similar to each other are omitted and only the highest-scoring version is depicted. As a reference, β''-alumina and NaSICon are included in bold as well; the NaRES structure discussed in the text is omitted since the score was comparably low (rare earths, 1D conduction). The column 'lit' describes where the structure was determined.

Formula	ICSD-#	sr	dm	sy	ms	oc	cr	pr	de	sum	notes	lit
$Na_{1.68}Al_{11}O_{17}$	201178	5	3	4	3	5	5	3	2	**35**	**β''-alumina**	[37]
$Na_8(AlSiO_4)_6(NO_3)_2$	413038	4	5	5	4	1	3	3	4	34	unstable, single O ion in the structure	[38]
$Na_{3.05}Zr_2Si_{2.05}P_{0.95}O_{12}$	62383	2	5	4	5	3	3	2	2	**31**	**NaSICon**	[24]
$NaAl(SiO_4)$	34884	4	5	5	1	1	3	3	4	31	determined at 750 °C	[39]
$Na_2(Al_2Si_3O_{10})$	83013	3	5	2	2	3	3	3	4	30	determined at 550 °C; shows void clusters	[40]
$Na(AlSiO_4)$	85553	5	1	4	4	1	3	3	3	29		[41]
$Na_2FeTi(PO_4)_3$	92226	3	5	5	1	1	4	2	3	29	described as Na ion conductor	[42]
$Na_2(Al_2Si_3O_{10})$	157309	5	1	1	5	3	3	3	3	29	theoretical structure	[43]
$NaOs_2O_6$	246504	3	5	5	5	1	4	0	0	28	theoretical structure	[44]
$Na_{3.70}Ca_{1.15}Ge_3O_9$	65017	2	5	5	4	2	3	0	2	28		[45]
$Na_{1.72}(Cr_{1.71}Ti_{6.29})O_{16}$	79502	5	1	3	1	5	3	3	2	28	described as Na ion conductor	[46]
$Na_{7.85}Al_{7.85}Si_{8.15}O_{32}$	108334	4	1	4	1	4	3	3	3	28	determined at 100 °C	[47]
$Na_{7.85}Al_{7.85}Si_{8.15}O_{32}$	108387	2	5	4	1	2	3	3	3	28	determined at 600 °C	[47]
$Na_{2.62}V_2(PO_4)_2(O_{1.6}F_{1.4})$	191947	4	3	3	2	4	3	1	3	28	described as Na insertion compound	[48]
$Na_5(MnO_4)$	47101	5	3	2	1	1	5	2	3	27		[49]
$Na_2(Al_2Si_3O_{10})$	160820	5	1	1	5	1	3	3	3	27	determined at 500 °C	[50]
$Na_2TiOSi_4O_{10}$	16899	4	1	3	4	1	3	3	3	27		[51]
$Na_2Mg_3Zn_2(Si_{12}O_{30})$	77121	4	1	4	1	3	2	4	3	27		[52]
$Na_{1.92}(Al_2Si_3O_{10})$	83012	5	1	1	5	1	3	3	3	27	determined at 300 °C	[39]
$Na_{1.78}(Mg_{1.87}Al_{0.13})(Si_2O_7)$	92968	5	3	4	1	2	2	2	3	27	high-pressure synthesis	[40]

CRYSTAL Research&Technology

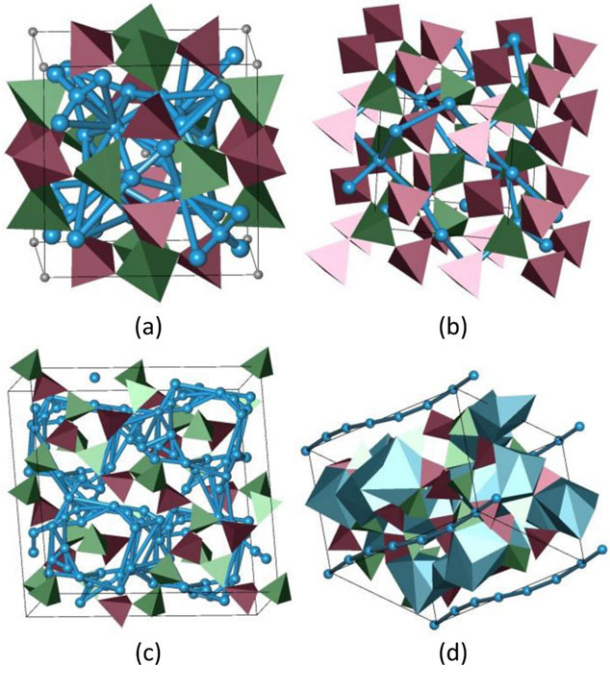

Fig. 4 The four highest scoring materials according to the algorithm used. All of them are aluminosilicates (red tetrahedra: AlO_4, green tetrahedra: SiO_4, blue polyhedra: NaO_x; grey atoms: O; blue atoms and bonds: identified void networks). (a) ICSD-# 413038 with the single O ions inside of the spherical conduction channel; b) ICSD- #34884, c) # 83013, d) # 85553.

β''-alumina ICSD- # 62383 and NaSICon (# 201178) structure was identified. The $Na_{1.72}(Cr_{1.71}Ti_{6.29})O_{16}$ phase (# 79502), with a score of 28, has an ion conductivity of $2 \cdot 10^{-5}$ S/cm at room temperature and an extrapolated ion conductivity of around $3 \cdot 10^{-2}$ S/cm at 300 °C [17]. The ion conductivity is lower than 0.1 S/cm, the value of the best reference material β''-alumina with a score of 35, but large enough for a good Na-ion conductor, which we predict for a material with a score of 28. The room temperature ion conductivity differs slightly (one order) from the expected value range as a result of the higher activation energy compared to β''-alumina.

The four highest-scoring materials are depicted in figure 4. For some compounds, we still observe void clustering (figure 4c). Its magnitude is considerably decreased by the new algorithm, though.

The highest-scoring material is $Na_8(AlSiO_4)_6(NO_3)_2$ (ICSD-# 413038) but it is questionable if this compound would be suitable, since a single oxygen ion is situated in the middle of an aluminosilicate sphere that hosts the detected Na^+ conductivity (see figure 4a). In the static case, where no ions move during the conduction process, this is not a problem, but a lone oxygen ion is very unlikely to be stable. The second-best-scoring compounds are aluminosilicates, as well. Especially $NaAlSiO_4$ (ICSD-# 34884) looks very promising, but was recorded at 750 °C.

For compounds recorded at elevated temperatures, it remains unknown how equivalent room temperature phases are in terms of structure. If the phase is still stable at other temperatures, the temperature coefficient will change unit cell dimensions only. Especially in high-temperature Na-S and Zebra cells the temperature is above 300 °C, in which case these high-temperature materials could be interesting. In the case of a phase transition or the movement of structural motifs, these newer structures would have to be (re)determined in order to analyse them with VDP again. The same would be valid for higher-pressure and calculated compounds. Eventually, only the actual experiment with these materials will show if a high Na^+ conductivity can be achieved.

Promising materials should be neither very simple (few atoms in small, very symmetric unit cells without any structural disorder) nor very complex compounds (large unit cells with many atoms and a high degree of structural disorder). A certain degree of complexity is necessary, especially to build up stable matrices. The conduction path itself should allow for a 'liquid-like' behaviour of to-be-conducted ions.

5 Conclusion

Voronoi-Dirichlet partitioning describes the conduction mechanism in the three best-known and best-conducting crystalline solid Na electrolytes: β''-alumina, NaSICon and NYS. The path geometry data of these materials was used for the VDP approach and applied to all ICSD entries comprising at least Na and O. Out of the 402 results, not only well-known conductors but also new potential solid Na electrolytes were identified. In order to reduce the complexity — all materials are deemed promising after the last step — we calculated crystallographic and economic parameters from the structural data. A weighting and scoring scheme was introduced to point towards the most promising compounds. Especially aluminosilicates and transition metal oxides could be thus identified.

Due to its simple algorithm, the methodology can be easily applied to large structural databases to calculate all important data in a very short time even on desktop and laptop computers without the use of large CPU power. It is therefore a very fast, high-throughput data mining routine. A disadvantage of the methodology is that it is only applied to static crystal structures

and that no direct energetic evaluation is possible. This could be done using bond-valence energy-landscape calculations [53] and/or density functional theory computations. In this way especially high-temperature and high-pressure compounds and candidates, where the conduction path does not lead through the crystal via structure-immanent Na ions, can be analysed. Future VDP approach improvements include the introduction of soft sphere considerations in the channel between voids and combinations with bond-valence and DFT methodologies.

Acknowledgements. We thank W. Neumann and K.-W. Benz for the kind invitation to contribute to the '50 years of Crystal Research and Technology' special issue and their long-term work as editors as well as to the referees for their time and valuable comments for improving the manuscript.

This work was financially supported by the German Federal Ministry for Economic Affairs and Energy (BMWi) within the joint research project 'BaSta' (0325563D), the German Federal Ministry of Education and Research (BMBF) within the joint research project 'CryPhysConcept' (03EK3029A) and 'SyNeSteSia' (05K14OFA), which is coordinated by A. Vyalikh. V. A. B. and A. P. S. thank the Russian Government (Grant 14.B25.31.0005) and the Russian Foundation for Basic Research (Grant 14-03-97034) for support.

F. M. wants to thank Carsten Richter for his programming support.

Key words. solid electrolyte, sodium battery, Voronoi-Dirichlet.

References

[1] https://yearbook.enerdata.net/world-electricity-production-map-graph-and-data.html

[2] Report D289: Advanced Energy Storage Technologies, Frost & Sullivan (2004).

[3] Global Materials Market for Alternative Energy Storage Mechanisms, 9833–39, Frost & Sullivan (2011).

[4] S. Glöser, L. T. Espinoza, C. Gandenberger, and M. Faulstich, Resour. Policy **44**, 35 (2015).

[5] P. Arora and Z. Zhang, Chem. Rev. **104**, 4419 (2004).

[6] K. Buß, P. Wrobel, and C. Doetsch, Int. J. Sust. Energy Plan. Manage. **9**, 31 (2016).

[7] J. T. Kummer and W. Neill, 'Battery having a molten alkali metal anode and a molten sulfur cathode' (1968), US Patent 3,413,150.

[8] Y.-F. Y. Yao and J. T. Kummer, J. Inorg. Nucl. Chem. **29**, 2453 (1967).

[9] Z. Yang, J. Zhang, M. C. W. Kintner-Meyer, X. Lu, D. Choi, J. P. Lemmon, and J. Liu, Chem. Rev. **111**, 3577 (2011).

[10] T. Oshima, M. Kajita, and A. Okuno, Int. J. Appl. Cer. Technol. **1**, 269 (2004).

[11] K. B. Hueso, M. Armand, and T. Rojo, Energy Environ. Sci. **6**, 734 (2013).

[12] T. Nestler, R. Schmid, W. Münchgesang, V. Bazhenov, J. Schilm, T. Leisegang, and D. C. Meyer, AIP Conf. Proc. **1597**, 155 (2014).

[13] M73D-39, Chemicals and Materials Market in Smart Grid Infrastructure: Smart E-Meters and HVDC Cable Materials to Drive Growth, Frost & Sullivan (2012).

[14] H. Böhm, Materials for high-temperature batteries, edited by C. Daniel and J. O. Besenhard, Handbook of Battery Materials (Wiley-VCH, Weinheim, 2011), chap. 21.

[15] B. Dunn, H. Kamath, and J.-M. Tarascon, Science **334**, 928 (2011).

[16] M. Avdeev, V. B. Nalbandyan, and I. L. Shukaev, Alkali Metal Cation and Proton Conductors: Relationships between Composition, Crystal Structure, and Properties, edited by V. V. Kharton, Solid State Electrochemistry I: Fundamentals, Materials and their Applications (Wiley VCH, Weinheim, 2009), chap. 7.

[17] S. Yoshikado, Y. Michiue, Y. Onoda, and M. Watanabe, Solid State Ionics **136–137**, 371 (2000).

[18] G. C. Farrington and J. L. Briant, Science **204**, 1371 (1979).

[19] A. V. Virkar, G. R. Miller, and R. S. Gordon, J. Am. Ceram. Soc. **61**, 250 (1978).

[20] H. Engstrom, J. B. Bates, W. E. Brundage, and J. C. Wang, Solid State Ionics **2**, 265.

[21] X. Lu, G. Xia, J. P. Lemmon, and Z. Yang, J. Power Sources **195**, 2431 (2010).

[22] http://ionotec.com/conductive-ceramics.html

[23] J. B. Goodenough, H. Y.-P. Hong, and J. A. Kafalas, Mat. Res. Bull. **11**, 203 (1976).

[24] J. P. Boilot, G. Collin, and Ph. Colomban, J. Solid State Chem. **73**, 160 (1988).

[25] H. U. Beyeler and T. Hibma, Solid State Commun. **27**, 641 (1978).

[26] F. Meutzner, W. Münchgesang, N. A. Kabanova, M. Zschornak, T. Leisegang, V. A. Blatov, and D. C. Meyer, Chem. Eur. J. **21**, 16601 (2015).

[27] V. A. Blatov, Crystallogr. Rev. **10**, 249 (2004).

[28] V. A. Blatov, A. P. Shevchenko, and D. M. Proserpio, Cryst. Growth Des. **14**, 3576 (2014).

[29] N. A. Anurova, V. A. Blatov, G. D. Ilyushin, O. A. Blatova, A. K. Ivanov-Schitz, and L. N. Dem'yanets, Solid State Ionics **179**, 2248 (2008).

[30] V. A. Blatov, G. D. Ilyushin, O. A. Blatova, N. A. Anurova, A. K. Ivanov-Schits, and L. N. Dem'yanets, Acta Cryst. B **62**, 1010 (2006).

[31] R. A. Huggins, Very Rapid Transport in Solids, edited by A. S. Nowick and J. J. Burton, Diffusion in Solids: Recent Developments (Academic Press, 1975, New York, San Francisco, London), chap. 9.

[32] A. Belsky, M. Hellenbrandt, V. L. Karen, and P. Luksch, Acta Cryst. B **58**, 364 (2002).

[33] O. A. Smirnova, R. O. Fuentes, F. Figueiredo, V. V. Kharton, and F. M. B. Marques, J. Electroceram. **11**, 179 (2003).

[34] Y.-L. Shin and M.-Y. Yi, Solid State Ionics **132**, 131 (2000).

[35] T. Kawaguchi, K. Fukuda, K. Tokuda, M. Sakaida, T. Ichitsubo, M. Oishi, J. Mizuki, and E. Matsubara, Phys. Chem. Chem. Phys. **17**, 14064 (2015).
[36] R. Kirchheim, J. Non-Cryst. Solids **272**, 85 (2000).
[37] J. P. Boilot, G. Collin, Ph. Colomban, and R. Comes, Phys. Rev. B **22**, 5912 (1980).
[38] C. H. Rüscher, Th. M. Gesing, and J.-Chr. Buhl, Z. Kristallogr. **218**, 332 (2003).
[39] T. F. W. Barth and E. Posnjak, Z. Kristallogr. **81**, 376 (1932).
[40] W. H. Baur and W. Joswig, N. Jb. Miner. Mh **1996**, 171 (1996).
[41] V. Kahlenberg and H. Böhm, Am. Miner. **83**, 631 (1998).
[42] J. Isasi and A. Daidouh, Solid State Ionics **133**, 303 (2000).
[43] J. J. Williams, C. W. Smith, K. E. Evans, Z. A. D. Lethbridge, and R. I. Walton, Chem. Mater. **19**, 2423 (2007).
[44] R. Saniz and A. J. Freeman, Phys. Rev. B **72**, 024522 (2007)
[45] F. Nishi and Y. Takéuchi, Acta Cryst. C **44**, 1867 (1988).
[46] Y. Michiue and M. Watanabe, J. Solid State Chem. **116**, 296 (1995).
[47] P. Vuli and V. Kahlenberg, N. Jh. Miner. Abh. **189**, 197 (2012).
[48] P. Serras, V. Palomares, T. Rojo, H. E. A. Brand, and N. Sharma, J. Mater. Chem. A **2**, 7766 (2014).
[49] G. Brachtel, N. Bukovec, and R. Hoppe, Z. Anorg. Allg. Chem. **515**, 101 (1984).
[50] H.-W. Wang and D. L. Bish, Am. Miner. **93**, 1191 (2008).
[51] D. R. Peacor and M. J. Bürger, Am. Miner. **47**, 539 (1962).
[52] A. Wohlfahrt, Heidelberger Geowissenschaftliche Abhandlungen **92**, 1 (1998).
[53] S. Adams and R. Prasada Rao, Phys. Status Solidi A **208**, 1746 (2011).

